Revista Brasileira de Cartografia (2016), Nº 68/5: 957-964
Sociedade Brasileira de Cartografia, Geodésia, Fotogrametria e Sensoriamento Remoto
ISSN: 1808-0936

ASSESSMENT OF LANDSCAPE CHANGES IN THE ANAVILHANAS ARCHIPELAGO DURING THE FLOOD PEAK AND DROUGHT EVENTS IN THE RIO NEGRO, CENTRAL AMAZÔNIA, BRAZIL

Avaliação das Mudanças da Paisagem no Arquipélago de Anavilhanas durante os Eventos de Pico de Inundação e Seca no Rio Negro, Amazônia Central, Brasil

Raimundo Almeida-Filho[1], Yosio Edemir Shimabukuro[1] & Carlos Henrique Beisl[2]

[1]National Institute for Space Research – INPE
Remote Sensing Division – DSR
Av. dos Astronautas, 1758, Jd. Granja, CEP: 12227-010, São José dos Campos, SP, Brazil
rai@dsr.inpe.br; yosio@dsr.inpe.br

[2]Universidade Federal do Rio de Janeiro – UFRJ
Laboratório de Sensoriamento Remoto por Radar – LabSAR
Caixa Postal 68552, Rio de Janeiro, RJ, Brazil
beisl@labsar.coppe.ufrj.br

Received on August 12, 2015/ Accepted on April 2, 2015
Recebido em 12 de Agosto, 2015/ Aceito em 2 de Abril, 2015

ABSTRACT

This article estimates for the first time the extents of the landscape changes in the Anavilhanas Archipelago, as registered by satellite images acquired during the flood peak and drought events ever recorded in the Negro River (in Portuguese, "Rio Negro"). The Anavilhanas constitutes the second largest group of freshwater islands in the world, comprising a complex pattern of islands, channels, lagoons, swamps, beaches and sandbanks, which dramatically changes during the seasonal periods of high and low waters. The results showed that approximately 1,700 Km^2 of flooded area in the high water period were reduced by about 50% during the low water period, allowing the appearance of more than 800 Km^2 of beaches, sandbanks, and shallow submerged sandbanks. The extent of these seasonal landscape changes associated with the pulses of rising and descending waters are dominant environmental factors affecting the rich biota of the archipelago, which is refuge of a diversified fauna and flora. Therefore the generated maps can be useful information for the hydrological modelling studies and for environmental monitoring of the region.

Keywords: Landscape Change, Amazon River, Remote Sensing, Thematic Mapper, ALOS-PALSAR, Fraction Images.

RESUMO

Este artigo estima pela primeira vez as extensões das mudanças da paisagem no arquipélago de Anavilhanas, como registrado por imagens de satélite adquiridas durante os eventos de pico de inundação e seca registrados no Rio Negro. Anavilhanas constitui o segundo maior grupo de ilhas de água doce no mundo, compreendendo um padrão complexo de ilhas, canais, lagoas, pântanos, praias e bancos de areia, que muda drasticamente durante os períodos sazonais de alta e baixa das águas. Os resultados mostraram que aproximadamente 1.700 Km^2 de área inundada no período de alta das águas foram reduzidos em cerca de 50% durante o período de baixa das águas, permitindo o aparecimento de mais

de 800 Km² de praias, bancos de areia e restingas. A extensão dessas mudanças sazonais da paisagem associada com os pulsos de subida e descida das águas são fatores ambientais dominantes que afetam a rica biota do arquipélago, que é o refúgio de uma diversificada fauna e flora. Portanto, os mapas gerados podem ser informações úteis para os estudos de modelagem hidrológica e para o monitoramento ambiental da região.

Palavras chaves: Mudança da Paisagem, Rio Amazonas, Sensoriamento Remoto, Mapeador Temático, ALOS PAL-SAR, Imagens Fração.

1. INTRODUCTION

The Anavilhanas Archipelago is on the Negro River ("*Rio Negro*"), about 50 Km from its confluence with the Solimões River, in the heart of the Brazilian Amazônia (Figure 1). The second largest group of freshwater islands in the world, the Anavilhanas comprises an intricate pattern of islands, channels, lagoons, swamps, and partially submerged sandbanks, refuge for a diversified fauna and flora, protected by the Anavilhanas National Park.

From a geological point of view, the Anavilhanas Archipelago results from the neotectonic activity that prevails in the Central Amazon, which derives from a compressional interplate stress regime caused by the Mid Atlantic Ridge spreading and the concurrent resistance from the Nazca and Caribbean plates (MENDIGUREN & RITCHER, 1978). This neotectonic activity was responsible for the local arrangement of fault blocks, which funneled the river down into a passageway that constitutes the narrowest width of the lower Negro River (ALMEIDA-FILHO & MIRANDA, 2007). Partially blocked by this natural barrier, the river widens upstream, assuming the appearance of a lake (up to 20 km wide and 100 km long). Free space in a low energy environment has favored the deposition of sediments (mainly clay and silt) to form the Anavilhanas Archipelago.

The landscape in the Anavilhanas Archipelago changes dramatically during the seasonal periods of high and low waters of the Rio Negro. Floods cause the total or partial drowning of many islands, which begin to emerge with the receding waters, forming beaches and sandbanks. The cycles of flooding and drought constitute a dominant environmental factor affecting the rich biota of the region. They modify the landscape features and, consequently, the habitats in the area. Because it is a very remote region in the heart of the Amazonian rainforest, remote sensing is the most practical and effective way to map the landscape changes caused by the phenomena of rising and descending waters. Thus, the aim of this study was to assess the changes in the landscape features of the archipelago, during the seasonal pulses of rising and descending waters. To cope with this task, the study used different satellite images, which were acquired during the years 2009 (peak flood) and 2010 (peak drought) events ever recorded in the Rio Negro.

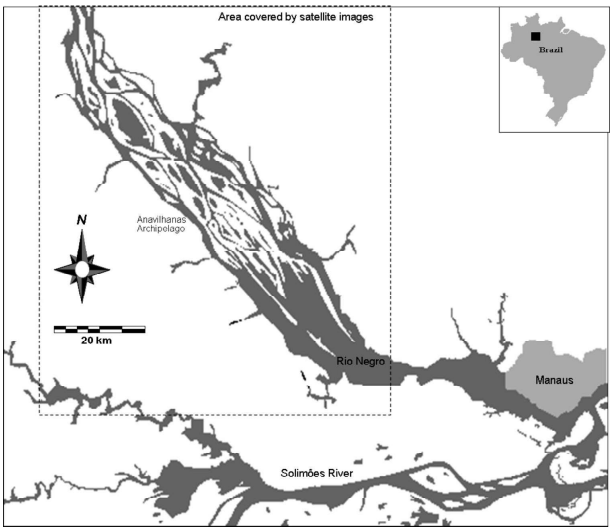

Fig. 1 - Location of the study area in the region of the Anavilhanas Archipelago, Central Amazônia.

2. RIO NEGRO HYDROLOGICAL CYCLE

The hydrological cycle of the Negro River features a period of rising waters levels, which peak between June and July, and by a period of falling water levels, which reach their lowest level between October and November (Figure 2). Figure 3 shows a historical time series of highest and lowest water levels for the Rio Negro, recorded in the port of Manaus. These figures show that over a period of 109 years the average difference in height of the water levels between the periods of high and low waters was 10.21 m. However, during the flood of 2009 and the drought of 2010, the Rio Negro broke its own historical records for peaks and droughts

(Marengo and Espinoza, 2016). On July 1st and 2nd 2009 the level of the river reached 29.77m, 7cm above the previous highest level in June 1953. Subsequently, on October 24th, 2010, the level fell to 13.63 m, 1cm below the previous minimum lowest, recorded in October 1963. The difference in the water level between these two events was of 16.14 m.

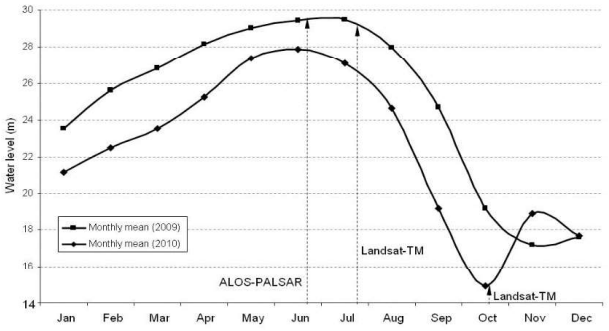

Fig. 2 - The hydrological cycles of the Negro River in 2009 and 2010 (data source: ANA, 2011). It also shows the TM and PALSAR acquisition dates.

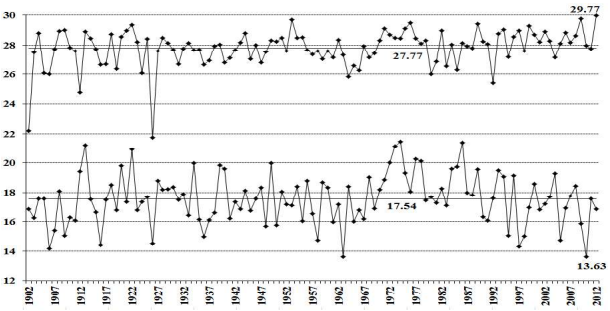

Fig. 3 - Historical time series of highest and lowest water levels for the Rio Negro recorded in the port of Manaus from the year of 1902 to 2012. The flood in July 2009 (29.77 m) and the subsequent drought in October 2010 (13.63 m) broke the previous records for flood and drought in July 1953 (29.70 m) and October 1963 (13.64 m), respectively (data source: ANA, 2011).

2010 is considered to have been the most severe drought ever registered in the Amazônia (LEWIS *et al.,* 2011), during which 38 municipalities in the region declared emergency situations (BALZA, 2010). The drought increased the incidence of landslides on the river banks, putting eleven municipalities at risk. As examples of these problems, an entire neighbourhood was struck in the town of São Paulo de Olivença, with an area of about 30,000 m^2 in the port of Manaus collapsed, throwing 68 large trucks and 56 containers into the river.

The wildlife also suffered the effects of this drought. Threatened species of manatees (*Trichechus inunguis*) and araú turtles (*Podocnemis expansa*), which Brazilian law has banned the hunting of since 1973, were confined to the lakes and intensively hunted in the municipalities of Manacapuru, Codajás, Silves, Tefé, and Autazes. The environmental police seized large amount of turtle eggs, as well as of protected fish species, such as arapaima (*Arapaima gigas*), tambaqui (*Colossoma macropomum*), peacock bass (*Cichla intermedia*), and so on (BRASIL, 2010).

3. SATELLITE IMAGES

To assess the landscape changes in the Anavilhanas Archipelago during the high and low water level stages on the Rio Negro, images from two different sensor systems were used: Thematic Mapper (TM) and Phased Array L-band Synthetic Aperture Radar (PALSAR). The TM onboard of the Landsat-5 satellite is a scanner system with a 30 m spatial resolution for the six reflective spectral bands distributed in the visible, near-infrared, and short wave infrared wavelengths and one thermal infrared band with 120 m spatial resolution (NOVO, 1989). The PALSAR *is* an L-band microwave system that was carried onboard of the Japanese *Advanced Land Observing Satellite* (ALOS). The ScanSAR mode used in this study has a ground spatial resolution of 100m (ROSENQVIST *et al.*, 2007).

The Landsat-TM images were acquired *on May 05, July 08, September 10 and 29 November 2009, and April 22, June 25 and October 31, 2010 during the period that occurred the flood peak (29.77m) in 2009 and* the minimum recorded level (13.63 m) in 2010. The *PALSAR* scene was also acquired during the high water period, on June 22, 2009. On that day, *the water level was only 0.12m below the peak recorded during the flood.*

3.1 Landsat TM image analysis

The multispectral images of the TM were converted into three endmember fraction images (ADAMS *et al.,* 1995; SHIMABUKURO & SMITH, 1991): green vegetation, soil, and

water. "Pure" pixels with spectral responses for these three endmembers were extracted from the bands 3 (0.63 – 0.69 μm), 4 (0.77 – 0.90 μm) and 5 (1.55 – 1.75 μm) from the TM. Represented by different proportions of vegetation, soil, and free-water within each pixel, the fraction images showed that the selected endmembers described the full range of natural variability of the ground features, it was attested by the very low values for the residual bands (the difference between measured and modelled spectral values in each band), and by fraction values that were neither less than 0 nor greater than 1. The Linear Spectral Unmixing approach is very appropriate for the study area since the land is covered mainly by water, vegetation and bare soil and the resulting fraction images highlight these targets on the ground. The multitemporal fraction images where analysed comparing to the River water level for the years of 2009 and 2010.

Based on the analysis of false colour composites of the fraction images with soil (R), vegetation (G), and water (B), four classes of land cover were elected to be mapped: water, vegetated island, sandbanks, and upland forest. After the multitemporal inspection, we decided to use the TM images acquired on May 05 and July 08, 2009 for the flood peak and TM image acquired on October 31, 2010 for the drought peak events. Due to the cloud cover in the images during the flood peak, we decided to use two TM images mentioned (May 05 and July 08, 2009). Then the vegetation, soil, and water fraction images from the three TM images were used to perform the multitemporal segmentation. This procedure generates the segmented objects that have changed during the time period studied and assures the accurate match between the polygons on the images acquired in different dates. Then these segmented objects are classified by a non-supervised classifier (ISOSEG) using the spectral information of the multitemporal images acquired during the flood peak and drought peak events. These classified objects are then labelled as the corresponding ground targets defined as a previous thematic classes (water, vegetated island, flooded forest, sandbanks, and upland forest). (ALMEIDA-FILHO & SHIMABUKURO, 2002) For flood period we used the fraction images corresponding to the TM image of May 05 and July 08, 2009 for classifying the segmented polygons; and for drought period we used fraction images derived from TM acquired on October 31, 2010. Finally the editing technique was performed in order to minimize the omission and commission errors in the digital classification (ALMEIDA-FILHO & SHIMABUKURO, 2002). It is done by overlaying the thematic classification over a RGB colour composite of the original TM images based on visual interpretation procedures. Therefore the proposed method produces classification maps with high accuracy similar to those obtained by visual interpretation.

3.2 Radar image analysis

Before processing, PALSAR image was resampled using nearest-neighbour interpolation to fit to the same spatial resolution of the Landsat-TM (30 m). Then, the scene was converted to the Universal Transverse Mercator (UTM) coordinate system, with scene-to-scene registration yielding accuracy of 1.6 pixels. During the high water period for the Amazonian rivers, vast areas of dense forest are flooded, but these areas are not detected by optical system like TM. However, radar images, especially those in the L-band frequency with more power to penetrate the vegetation canopy, allow the detection of these areas of flooded forest (HESS *et al.*, 1990).

Four dominant land cover classes were visually identified in the ScanSAR image over the Anavilhanas Archipelago: water, vegetated islands, upland forest, and flooded forests. Areas of water appears dark, due to the specular reflection of the incident radar beam on the smooth surface of the river; upland forest appears in intermediate grey shades, due to the radar backscatter by the forest canopy; and flooded forest appears in bright grey shades, due to the double-bounce reflections between smooth water surfaces underneath the forest canopy and tree trunks (HESS *et al.*, 1990).

The first step in the processing of the radar image was the application of an algorithm to correct the antenna pattern, followed by a Frost filter (FROST *et al.*, 1982) with a 3 x 3 window

size to reduce radar speckle. In addition, the scene was converted from amplitude data format to normalised radar cross section (σ^0), according to the equation (1) below (ROSENQVIST *et al.,* 2007):

$$\sigma^0 = 10 \times \log_{10}(DN)^2 + CF \qquad (1)$$

where CF = – 83.0 dB and DN is the Digital Number (Gray level)

To map and to estimate the extent of these four land cover classes, an unsupervised deterministic classifier algorithm (unsupervised semivariogram textural classifier - USTC) that combines both textural and radiometric information (MIRANDA *et al.,* 2004) was applied over the processed PALSAR image.

4. RESULTS AND DISCUSSION

Segmentation and region-classification of the fraction images allowed to estimating the extent and variation of the landscape features during high and low water periods in the Anavilhanas Archipelago for the first time. Figure 4 is a false-colour composite with soil (Red - R), vegetation (Green - G), and water (Blue - B) fraction images derived from the Landsat-TM scene and its corresponding land cover map. This map shows an area of water of about 1,700 Km^2, and a complex array of narrow, elongated islands with dense vegetation, which together cover approximately 380 Km^2.

Figure 5 shows the ALOS-PALSAR scene and its corresponding land cover map. Although the level of the Rio Negro was 0.36 m higher than on the date of the Landsat-TM acquisition, the area of open water in the radar image was about 3.5% lower than that mapped in the TM fraction images. One possible reason for this small difference is the poorer spatial resolution of the radar image in defining terrain features as precisely as TM images do. About 45% of the areas mapped as vegetated islands in the Landsat-TM fraction images were flooded forest in the radar scene, which covered about 415 Km^2. However, the final extent of the area of flooded forest was certainly higher, considering that after the acquisition of the radar image the water level rose by over 0.12

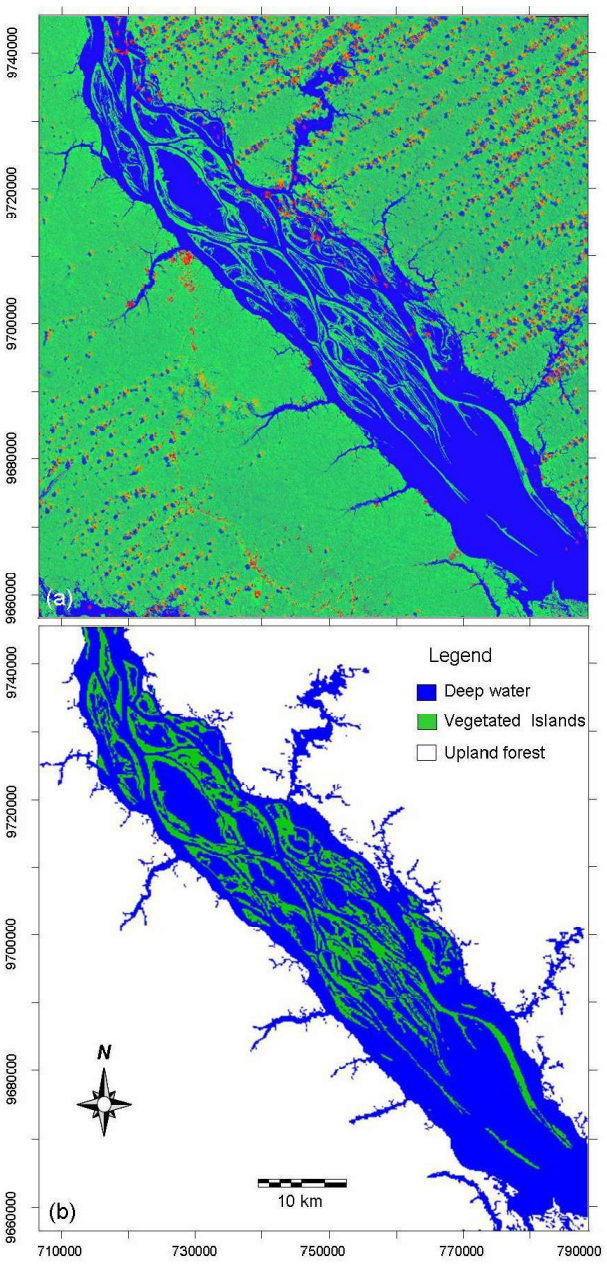

Fig. 4 - False-colour composite with soil (R), vegetation (G), and water (B) fraction images derived from the Landsat-TM scene (a) acquired during the 2009 flood period, and corresponding land cover map (b) of the Anavilhanas Archipelago. Coordinates are UTM/ SAD 69, Zone 20.

m to the peak of the flood (such an increase is significant considering the flat topography of the area). Together, the flooded area (water plus flooded forest) covered more than 2,000 Km^2, and certainly it was even larger during the peak of the flood on July 1st and 2nd. However, compared to the low water period, the flooded area was reduced by about 50%.

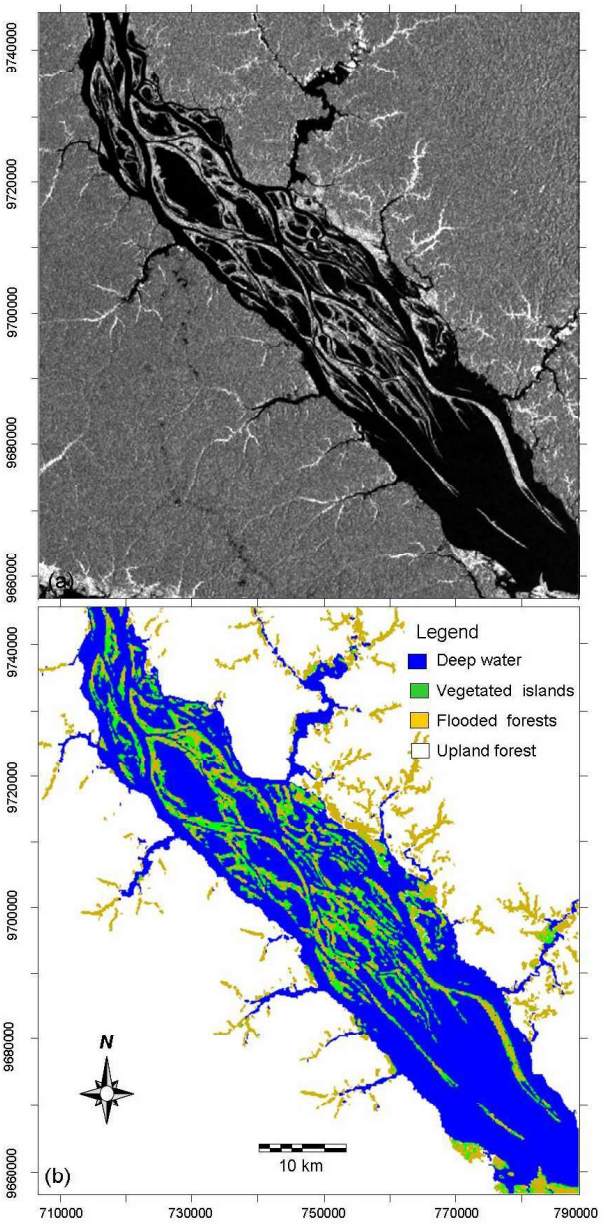

Fig. 5 - ALOS-PALSAR scene (a) acquired during the 2009 flood and corresponding land cover map (b) of the Anavilhanas Archipelago. Coordinates are UTM/SAD 69, Zone 20.

The area of water substantially decreased in the scene acquired during the period of receding waters, and covers a surface of only approximately 53% of that during the flood period (849 Km^2). The receding waters resulted in an increase of about 35% (from 380 Km^2 to 515 Km^2) in the areas of vegetated islands, compared to the period of high water. The drought also enabled the emergence of about 492 Km^2 of beaches and sandbanks and about 242 Km^2 of shallow submerged sandbanks. Despite occurring throughout the entire archipelago, shallow submerged sandbanks predominate in the central and in downstream portions of the archipelago. Figure 6 is a false-colour composite combining soil (R), vegetation (G), and water (B) fraction images derived from the TM image acquired on October 31, 2010, and its corresponding land cover map.

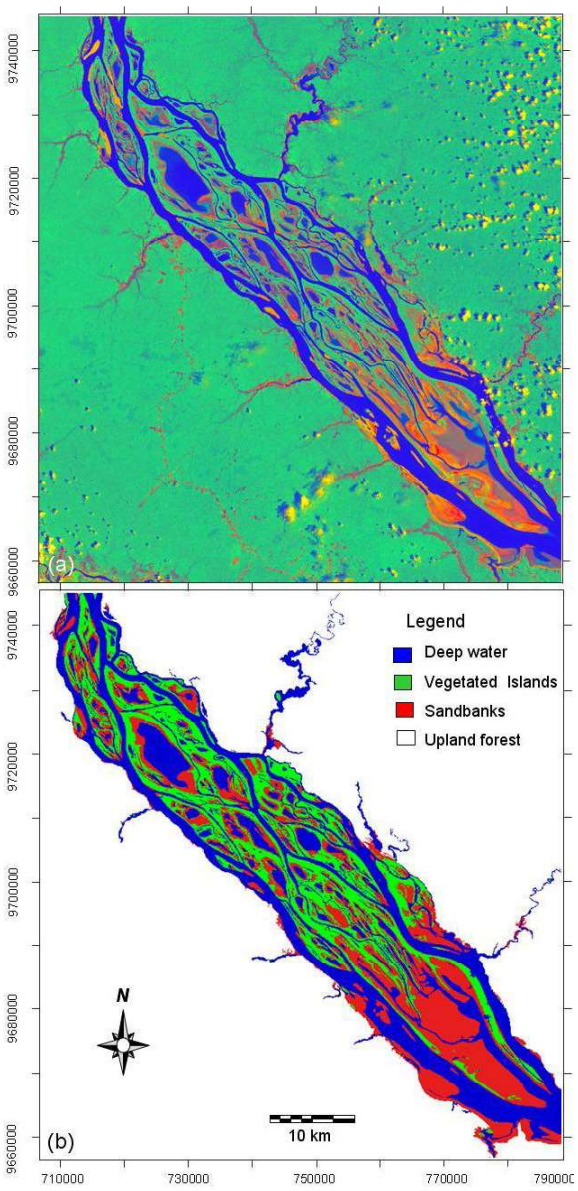

Fig. 6 - False-colour composite with soil (R), vegetation (G), and water (B) fraction images derived from the Landsat-TM scene (a) acquired during the 2010 receding period, and corresponding land cover map (b) of the Anavilhanas Archipelago. Coordinates are UTM/SAD 69, Zone 20 (see Figure 1 for location).

Table 1 summarizes the extent of the land cover classes in the area of the Anavilhanas Archipelago, as observed in the satellite images

acquired during the flood of 2009 (Landsat TM and PALSAR) and the drought of 2010 (Landsat TM).

Table 1: Extent (km^2) of the land cover types during flooding and drought in the rio negro region.

		Deep-water	Vegetated islands	Sand-banks	Flooded forest
TM 05 May and 08 Jul 2009	Flooding period	1,700	362	0	0
PALSAR		1,534	173	0	415
TM 31 Oct 2010	Drought period	905	390	794	0

4. CONCLUSIONS

The use of remote sensing images acquired by different satellites during the maximum flood and the maximum drought periods for the Negro River provided for the first time an estimation of the landscape features of the Anavilhanas Archipelago. Results showed that a surface of about 2,000 Km^2 entirely flooded during the high waters period is converted into about 1,200 Km^2 of vegetated islands, beaches, and shallow submerged sandbanks in the minimum level water event. The result obtained by the proposed approach can be an important source of information in the effort to better understanding aspects associated with the pulses of rising and receding waters. Therefore the generated maps can be useful information for the hydrological modelling studies and for environmental monitoring of the region.

REFERENCES

ADAMS, J. B.; SABOL, D.; KAPOS, V.; ALMEIDA-FILHO, R.; ROBERTS, D. A.; SMITH, M.O.; GILLESPIE, A. R. Classification of multispectral images based on fractions of endmembers: application to land-cover in the Brazilian Amazon. **Remote Sensing of Environment**, 52: 137-152, 1995.

AGÊNCIA NACIONAL DE ÁGUAS – ANA <http://www2.ana.gov.br/Paginas/default.aspx>. Accessed on January 21, 2011.

ALMEIDA-FILHO, R.; MIRANDA, F. P. Mega capture of the Rio Negro and formation of the Anavilhanas Archipelago, Central Amazônia, Brazil: evidences in a SRTM digital elevation model. **Remote Sensing of Environment**, 110: 387-392, 2007.

ALMEIDA-FILHO, R.; SHIMABUKURO, Y. E. Digital processing of Landsat-TM time-series for mapping and monitoring degraded areas caused by independent gold miners, Roraima State, Brazilian Amazon. **Remote Sensing of Environment**, 79: 42-50, 2002.

BALZA, G. **Rios Solimões e Amazonas têm maior seca da história**, <http://noticias.uol.com.br/cotidiano/ultimas-noticias/2010/10/22/rios-solimoes-e-amazonas-tem-maior-seca-da-historia.htm>. Accessed in 2010.

BRASIL, K. **Com a seca na Amazônia, tartarugas e peixes-boi viram alvo fácil de caçadores. Folha de São Paulo** <http://www1.folha.uol.com.br/fsp/cotidian/ff0111201008.htm>. Accessed on December 30, 2010.

FROST, V.S.; STILES, J. A.; SHAMMUNGAN, K. S.; HOLTZMAN, J. C. A model for radar images and its applications to adaptative digital filtering of multiplicative noise. **IEEE Transactions on Pattern Analysis and Machine Intelligence**, 4: 157-166, 1982.

HESS, L. L.; MELACK; J. M.; SIMONETT, D. S. Radar detection of flooding beneath the forest canopy: a review. **International Journal of Remote Sensing**, 11: 1313-1325, 1990.

LEWIS, S. L.; BRANDO, P. M.; OLIVER, L.; PHILLIPS, O. L.; GEERTJE, M. F.; HEIJDEN, G. M. F.; NEPSTAD, D. The 2010 Amazon drought. **Science**, 331: 554, 2011.

MARENGO, J. A.; ESPINOZA, J. C. Extreme seasonal droughts and floods in Amazonia: causes, trends and impacts. **International Journal of Climatology**, 36, 3, 1033-1050, 2016.

MENDIGUREN, J. A.; RITCHER, F. M. On the origin of compressional interplate stress in South America. **Physics of the Earth and Planetary Interiors,** 16, 318−326, 1978.

MIRANDA, F. P.; MENDONZA, A. A.; PEDROSO, E. C.; BEISL, C. H.; WELGAN, P.; MORALES, L. M. Analysis of RADARSAT-1 data for offshore monitoring activities in the Cantarell Complex, Gulf of Mexico, using the

unsupervised semivariogram textural classifier (USTC). **Canadian Journal of Remote Sensing**, 30: 424-436, 2004.

NOVO, E. M. L. M. **Sensoriamento Remoto: princípios e aplicações. São Paulo**. ed. Edgard Blücher, 308p, 1989.

ROSENQVIST, A.; SHIMADA, M.; ITO, N.; WATANABE, M. ALOS PALSAR: A Pathfinder Mission for Global-Scale Monitoring of the Environment. **IEEE Transactions on Geoscience and Remote Sensing**, 45: 3307-3316, 2007.

SHIMABUKURO, Y. E.; SMITH, J. A. The least squares mixing models to generate fraction images derived from remote sensing multispectral data. **IEEE Transactions on Geoscience and Remote Sensing,** 29, 1, 16-20, 1991.